stances $Mg_2Si$, $Mg_2Ge$, and $Mg_2Sn$ have resistivities in the "semiconducting" range, $10^{-1}$ to $10^4$ ohm cm. All of the new forms exhibit a markedly greater resistance to attack by moist air or dilute mineral acids than the parent materials.

P. Cannon
E. T. Conlin
*General Electric Research Laboratory, Schenectady, New York*

### References and Notes

1. G. C. Kennedy and P. N. LaMori, in *Progress in Very High Pressure Research*, F. P. Bundy, W. R. Hibbard, H. M. Strong, Eds. (Wiley, New York, 1961), p. 304.
2. F. P. Bundy, H. P. Bovenkerk, H. M. Strong, R. H. Wentorf, Jr., *J. Chem. Phys.* **35**, 383 (1961).
3. The most recent structure determination for regular $Mg_2Si$ and $Mg_2Ge$ is that of G. Busch and V. Winkler, *Helv. Phys. Acta*, **26**, 578 (1953); and for $Mg_2Sn$ that of E. Zintl and H. Kaiser, *Z. Anorg. Allegam. Chem.* **211**, 113 (1933).
4. We thank Mrs. D. K. deCarlo for her skilled assistance.

5 May 1964

## X-ray Diffraction Data on Two High-Pressure Phases of Calcium Carbonate

Abstract. *X-ray diffraction studies conducted at high pressure with a beryllium pressure vessel show that compression parallel to the* c*-axis of $CaCO_3$-I (calcite), as the phase boundary of $CaCO_3$-II (modified calcite type) is approached, results in a relative reduction of the* c*-axis of phase II of several times that of the* a*-axes. Such data are not consistent with previously proposed anion disorder in $CaCO_3$-II. At 18.7 ± .5 kb and room temperature a new phase of $CaCO_3$ has been observed that is assumed to be phase III found by Bridgman. At this pressure the x-ray diffraction pattern can be indexed as orthorhombic $KNO_3$-IV type, with $a_0 = 8.90 \pm .01$ Å, $b_0 = 8.42 \pm .01$ Å, and $c_0 = 7.14 \pm .01$ Å ($Z = 10$).*

The stability regions of $CaCO_3$-II and $CaCO_3$-III with respect to calcite ($CaCO_3$-I) have been worked out by Bridgman (*1*); it was his conclusion that both phases II and III were minor modifications of a calcite structure. Jamieson (*2*) also came to this conclusion from high-pressure x-ray studies of $CaCO_3$ for which he used a single crystal diamond bomb. Jamieson further suggested that the triangular carbonate groups of the phase II structure were in a state of rotational disorder similar to the high-temperature disorder transformations observed in the alkaline earth carbonates by Lander (*3*), and in $NaNO_3$ by Siegel (*4*). Until now, virtually nothing has been learned about the $CaCO_3$-III structure.

The apparatus used in the study reported here consisted of a supported beryllium pressure vessel modified for heating to 600°C. The vessel and press were mounted on the goniometer of a Norelco x-ray diffraction unit; diffraction patterns could thus be obtained from the sample while it was subjected to elevated temperatures and pressures. The vessel design and experimental procedure were described in detail previously (*5*). Pulverized Iceland spar (*6*) or synthetic reagent-grade $CaCO_3$, diluted with cornstarch (*7*), was compressed into thin (less than 1 mm) pellets for sample material.

One of the purposes of this study was to investigate further the possibility of rotational anion disorder in $CaCO_3$-II. In such a process all diffraction peaks with $l$ odd should disappear at the transition inasmuch as the $c$-axis of the original calcite structure would be halved. Lander (*3*) has shown that such disorder exists in the aragonite-type alkaline-earth carbonates and with increasing temperature results in a marked expansion of the direction ($c$-axis) normal to the carbonate layers of the structure. Siegel (*4*) also recognized anion disorder in calcite-type $NaNO_3$ with similar expansion of the $c$-axis (also the direction normal to the anion layers in this structure). This expansion is proportionally much greater than the expansion along other axial directions in these structures, and appears to result from electrostatic repulsion of oxygen ions in "overlap" with cations or other oxygen ions as rotation of the anion groups takes place (*3*, p. 899).

If such disorder exists in $CaCO_3$-II, as Jamieson suggests, then one would expect expansion along the $c$-axis either at the transition point or as the transition point is approached, depending on whether the transformation is abrupt or gradual.

Therefore, several records of the 113 peak of calcite were obtained with increasing pressure up to 15.5 kb at which time this peak could no longer be detected. The transition pressure measured by Bridgman (*1*) is 14.6 kb. The 113 peak was easily recognized at 3.5, 7, and 11 kb. In addition to the loss of 113, a marked difference in the amount of shifting of the 104 and 006 peaks was observed. These data, given in terms of $\Delta 2\theta$ and $\Delta d$ for one of the experiments, are presented in Table 1, and demonstrate a large contraction of the $c$-axis relative to the $a$-axes, rather than expansion. To interpret the data in Table 1 correctly, one should recognize that, for a hexagonal crystal, if $(\Delta c/c_0) \geqq (\Delta d/d_0)_{h0l}$ then $(\Delta a/a_0) \leqq (\Delta d/d_0)_{h0l} \leqq (\Delta c/c_0)$, regardless of the values of the indices $h$ and $l$ (except that they are not both zero). It is also important to note that

$$\lim_{\frac{h}{l} \to 0} \left( \frac{\Delta d}{d_0} \right)_{h0l} = \frac{\Delta c}{c_0}$$

and that

$$\lim_{\frac{l}{h} \to 0} \left( \frac{\Delta d}{d_0} \right)_{h0l} = \frac{\Delta a}{a_0}$$

For the present case not only is $d_{006}$ smaller than $d_{104}$ (as shown by the negative values of the right-hand column of Table 1) but the decrease in $d_{006}$ is

Table 1. Effect of pressure on the differences in Bragg angle and interplanar spacings for 104 and 006 of calcite.

| Internal pressure (kb) | $2\theta_{006} - 2\theta_{104}$ (deg. MoK$\alpha$) | $d_{006} - d_{104}$ (Å) |
|---|---|---|
| 0 | 0.88 | −0.092 |
| 3.5 | 0.92 | −0.096 |
| 7 | 0.93 | −0.097 |
| 11 | 0.95 | −0.099 |
| 15.5 | 1.02 | −0.106 |

Table 2. X-ray diffraction data for $CaCO_3$-III at 18.7 ± 0.5 kb and 25°C.

| *hkl* | $d_{\text{obs.}}$ Å | $d_{\text{calc.}}$ Å | $I/I_0$* |
|---|---|---|---|
| 020† | 4.22 | 4.21 | 10 |
| 002† | 3.57 | 3.57 | 20 |
| 220 | 3.02 | 3.06 | 100 |
| 030† | 2.81 | 2.81 | 100 |
| 212 | 2.65 | 2.64 | 5 |
| 131 | 2.53 | 2.51 | 10 |
| 230† | 2.37 | 2.37 | 15 |
| 302 | 2.28 | 2.28 | 10 |
| 400† | | 2.23 | |
| 023 | 2.08 | 2.07 | 5 |
| 223 | 1.88 | 1.88 | 2 |
| 402† | | 1.89 | |
| 313 | 1.81 | 1.81 | 10 |
| 042 | | 1.81 | |
| 033† | | 1.81 | |
| 412† | | 1.84 | |
| 051 | 1.64 | 1.64 | 5 |
| 520 | | 1.64 | |
| 024 | | 1.64 | |

* Relative heights of the peaks. † Indices in common with pattern for $KNO_3$-IV.

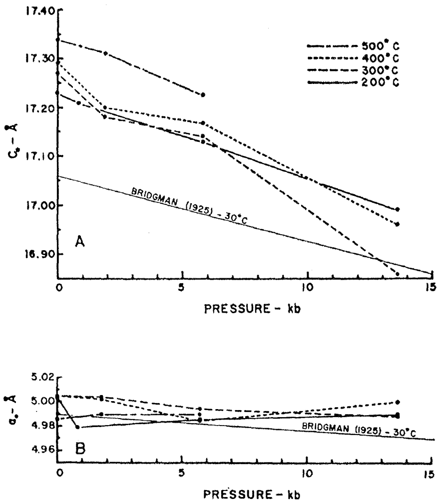

Fig. 1. (*A*) Plot of $c_0$ of $CaCO_3$-I versus pressure for various temperatures. Pressures given are obtained from prior vessel calibration. MoK$\alpha$ radiation. Supported beryllium pressure-vessel. (*B*) Plot of $a_0$ of $CaCO_3$-I versus pressure for various temperatures. Pressures given are obtained from prior calibration of the vessel. MoK$\alpha$ radiation. Supported beryllium pressure-vessel.

greater than the decrease in $d_{104}$ for a given increment of pressure. Therefore,

$$\left(\frac{\Delta d}{d_0}\right)_{006} = \frac{\Delta c}{c_0} > \left(\frac{\Delta d}{d_0}\right)_{104} > \frac{\Delta a}{a_0}.$$

The probable error for the spacing differences of Table 1 is judged to be ± 0.005 Å and is less than that for a direct measurement of spacings. The measurement of differences results in the elimination of several sources of error. In one experiment, however, $a_0$ and $c_0$ were determined directly by use of internal standards. Thus, for $CaCO_3$-II at 15.5 ± 1 kb and 25°C these values are $a_0 = 4.98 \pm 0.01$ Å, and $c_0 = 16.83 \pm 0.02$ Å. The cell constants of calcite at room temperature and pressure are $a_0 = 4.989$ Å, and $c_0 = 17.062$ Å (*8*). If it is assumed that the change in $a_0$ at 15.5 kb is 0.01 Å, the compression parallel to $c$ is over six times that parallel to $a$. Bridgman (*9*) previously measured the compression of calcite single crystals in directions normal to and parallel to the $c$-axis up to 11.8 kb at 30°C. If it is assumed that his compression equations hold to 15.5 kb, the cell constants for $CaCO_3$-II are calculated to be $a_0 = 4.97$ Å and $c_0 = 16.82$ Å; these values take into account the 0.00135 cm$^3$/g volume change at the I–II transition found by Bridgman (*1*) at 14.6 kb.

An attempt to measure the variation in compressibility of calcite with temperature by means of this apparatus has resulted in data of insufficient accuracy for the purpose intended, but the cell constants derived show clearly the large change in $c_0$ relative to $a_0$ of calcite. The results of this study are shown in Fig. 1, *A* and *B*. The constants were obtained from a least squares analysis of the 104, 110, 113 (when present), 108, and 116 peaks of the diffraction pattern. Also included in Fig. 1 are the corresponding curves for 30°C calculated from Bridgman's compression equations

$$-\frac{\Delta l}{l_0} = 8.071 \times 10^{-6}P - 3.26 \times 10^{-12}P^2 \quad \text{(parallel to } c_0\text{)}$$

and

$$-\frac{\Delta l}{l_0} = 2.668 \times 10^{-6}P - 0.70 \times 10^{-12}P^2 \quad \text{(normal to } c_0\text{)}$$

where $l_0$ is an increment of length at atmospheric pressure, and $P$ is in kilograms per square centimeters. Figure 1 shows that the slopes of the curves at the higher temperatures do not differ much from those of 30°C. The approximate slope of all the curves of Fig. 1*A* is −0.027 Å/kb, whereas the average slope of those of Fig. 1*B* is very close to zero (Bridgman's curves excluded).

The above results show that formation of phase II from phase I involves a considerable reduction in $c_0$ compared with $a_0$. From this fact, and from the findings of Lander and Siegel, it is now doubtful that anion rotation can be the mechanism of transformation of phase I to phase II. Such disorder results in $c$-axis expansion, not contraction. As an alternative, it is suggested here that $CaCO_3$-II might be isostructural with $KNO_3$-III; the latter phase is also a minor variation of the calcite structure (*10*). Several arguments are presented by Davis (*11*) in support of this correlation, three of which will be mentioned here. First, $KNO_3$-III occupies a position in the $KNO_3$ phase diagram analogous to that of $CaCO_3$-II in the $CaCO_3$ phase diagram, both being separated from phases of the aragonite-type by a *P-t* boundary of negative slope. Secondly, in going from phase I of $KNO_3$ (disordered calcite type) to phase III (also a modified calcite type) with increasing pressure there is observed a large compression of the $c$-axis relative to the $a$-axes. Thirdly, the two x-ray diffraction patterns can be indexed identically on the basis of the calcite-type hexagonal "pseudo-cell" with no peaks indexed with $l$ odd. Although $KNO_3$-III has an ordered calcite-like structure, Barth (*12*) proposes that the $NO_3^-$ ion is displaced from the cell center along the $c$-axis by 6 percent of the length of the $c$-axis.

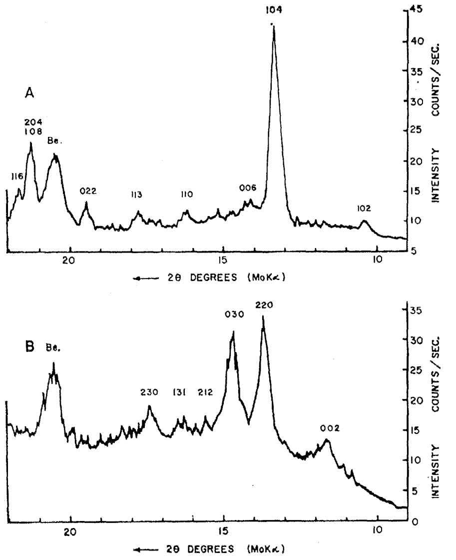

Fig. 2. (*A*) X-ray diffraction pattern of $CaCO_3$-I at room temperature and pressure. The pattern of phase II is the same, except that it lacks the weak 113 peak. MoK$\alpha$ radiation. Supported beryllium pressure vessel. Beryllium peak from vessel wells labeled Be. (*B*) X-ray diffraction pattern of $CaCO_3$-III at room temperature and 18 ± 2 kb. MoK$\alpha$ radiation. Supported beryllium pressure vessel. Beryllium peak from walls of vessel labeled Be. Pattern traced directly from record and left uncorrected for shift in the height of the sample.

At higher pressures (up to 27 kb) several new diffraction peaks appeared and are considered to represent Bridgman's phase III. The transition pressure given by him is 17.7 kb at 25°C (*1*), and values determined here by two different methods are 17.0 ± 0.3 kb and 18.7 ± 0.5 kb. The diffraction patterns of $CaCO_3$-I and $CaCO_3$-III taken through the pressure vessel are presented in Fig. 2 and the diffraction data in Table 2. The pattern can be indexed as orthorhombic $KNO_3$-IV type (*10, 11, 13*) with constants $a_0 = 8.90 \pm 0.01$ Å, $b_0 = 8.42 \pm 0.01$ Å, and $c_0 = 7.14 \pm 0.01$ Å ($Z = 10$ molecules per cell) at 18.7 ± 0.5 kb and 25°C. In fact, by comparing the phase diagrams of $CaCO_3$ and $KNO_3$, and from the x-ray diffraction evidence presented here, it is a distinct possibility that the various phases of these two compounds are completely isostructural. Nevertheless, the inherent limitations of the powder method and the few diffraction peaks obtained thus far for $CaCO_3$-III prohibit a definite conclusion. The phase III peaks, however, have been observed in eight independent experiments, and records taken at intervals of pressure and time show with certainty that the transformation is reversible.

The specific volume of CaCO$_3$-III at 18.7 ± 0.5 kb and 25°C is 0.315 ± .002 cm$^3$/g. Taking the specific volume of phase II at 15.5 ± 1 kb (transformation pressure I–II) and the same temperature to be 0.360 ± .002 cm$^3$/g the value for $\Delta v$ is $-0.045$ cm$^3$/g. This is the volume change for the II–III transition as well as that due to any compression that may occur in the interval between 15.5 and 18.7 kb. However, Bridgman (*1*) determined the II–III decrement alone to be $-0.00956$ cm$^3$/g and, because of the unknown compressibility in the interval 15.5 to 18.7 kb, a direct comparison of the two decrements cannot be made.

B. L. DAVIS*
*Institute of Geophysics and Planetary Physics, University of California, Los Angeles*

**References and Notes**

1. P. W. Bridgman, *Am. J. Sci.* **237**, 7 (1939).
2. J. C. Jamieson, *J. Geol.* **65**, 334 (1957).
3. J. J. Lander, *J. Chem. Phys.* **17**, 892 (1949).
4. L. A. Siegel, *ibid.*, p. 1146.
5. B. L. Davis and L. H. Adams, *J. Phys. Chem. Solids* **25**, 379 (1964).
6. Ward's collection.
7. It was observed during the study that the addition of cornstarch to the CaCO$_3$ aided in the conversion of phase I to phase III. The action is not considered to be catalytic, but is perhaps related to the flow in the sample as high pressures are applied.
8. H. E. Swanson and R. K. Fuyat, *Natl. Bur. Stand. U.S. Circ.* **539** (II), 51 (1953).
9. P. W. Bridgman, *Am. J. Sci.* **10**, 483 (1925).
10. B. L. Davis and L. H. Adams, *J. Phys. Chem. Solids* **24**, 787 (1963).
11. B. L. Davis, thesis, Univ. of California, Los Angeles (1964).
12. T. F. W. Barth, *Z. Physik. Chem. Leipzig* **43**, 448 (1939).
13. B. L. Davis and L. H. Adams, *Z. Krist.* **117**, 399 (1962).
14. Publication No. 359, Institute of Geophysics and Planetary Physics, University of California, Los Angeles. Supported by grants from the National Science Foundation. I acknowledge the assistance and helpful suggestions of Drs. L. H. Adams and W. E. Sharp. Dr. Sharp also performed the least squares analysis of the CaCO$_3$-II cell constants at the U.C.L.A. computing facility.

* Present address: Department of Geology and Geological Engineering, South Dakota School of Mines and Technology, Rapid City.

10 April 1964

# Tryptophan Synthetase from Neurospora: A Modification in the Reaction Scheme

Abstract. *In addition to indole-3-glycerolphosphate, an unreported reaction product has been detected in incubation mixtures containing tryptophan synthetase from* Neurospora, *indole, and glyceraldehyde-3-phosphate. This product has been tentatively identified as an indole derivative. Since this compound is not formed in incubation mixtures initially containing only enzyme and indole-3-glycerolphosphate, it was concluded that indole-3-glycerolphosphate synthesis and breakdown are not simply the forward and reverse components of a reversible reaction.*

Tryptophan synthetase from both *Neurospora crassa* and *Escherichia coli* has proven extremely useful in genetic and enzymatic studies (*1, 2*). In interpreting the relation between gene and enzyme in these systems it is important that all the reactions catalyzed by tryptophan synthetase be well understood. The reactions catalyzed by this enzyme are believed to be:

$$\text{Indole-3-glycerolphosphate plus L-serine} \rightarrow \text{L-tryptophan plus D-glyceraldehyde-3-phosphate.} \quad (1)$$

$$\text{Indole} + \text{L-serine} \rightarrow \text{L-tryptophan} + \text{water.} \quad (2)$$

$$\text{Indole-3-glycerol phosphate} \underset{(R)}{\overset{(F)}{\rightleftharpoons}} \text{indole plus D-glyceraldehyde-3-phosphate} \quad (3)$$

where F and R mean forward and reverse. Reactions 1 and 2 require pyridoxal phosphate and essentially are irreversible. Reaction 3, the reaction considered in this report, was believed to be reversible, with the forward reaction (3F) accelerated by pyridoxal phosphate and the reverse reaction (3R), by pyridoxal phosphate and L-serine. Garrick and Suskind (*3*) have noted discrepancies in reaction 3 which are not readily compatible with its formulation as simply the reversible interconversion of indole-3-glycerolphosphate to indole plus D-glyceraldehyde-3-phosphate. The detection of an indole derivative is reported here for reaction mixtures which initially contain tryptophan synthetase, indole, and glyceraldehyde-3-phosphate (reaction 3R), but not for mixtures that initially contain the enzyme and indole-3-glycerolphosphate (reaction 3F).

A lack of stoichiometry between the disappearance of indole and the formation of indole glycerolphosphate (reaction 3R) had been noted earlier for extracts of *Neurospora* tryptophan synthetase mutant td$_2$ (*4*) and for *Escherichia coli* extracts (*5*). Garrick and Suskind (*3*), after observing different rates for tryptic inactivation of reactions 3F and 3R, examined the stoichiometry for both reactions. The nonstoichiometric relation of indole and indole glycerolphosphate in reaction 3R was confirmed with highly purified extracts of wild-type *Neurospora* tryptophan synthetase, and a nonstoichiometric relation of the two compounds was also observed for reaction 3F (*3*). Data from fractionations, a survey of *Neurospora* tryptophan synthetase mutants (*3*) and quantitative precipitin tests (*6*) eliminated the possibility that the two reactions, 3F and 3R, were catalyzed by separate proteins. Since the activity of reaction 3F was markedly inhibited and precipitated by antibody to the enzyme, and reaction 3R activity was precipitated, but not specifically inhibited by the antibody (*3*), it is possible that reactions 3F and 3R are reactions occurring at different sites on the tryptophan synthetase protein, or that there is differential accessibility of each substrate to the active center in the presence of antibody.

We have examined reaction mixtures which initially contained tryptophan synthetase, indole, and glyceraldehyde-3-phosphate for the presence of reaction products other than indole glycerolphosphate. An enzymatically synthesized indole derivative, not identical to indole, indole glycerolphosphate, indole-3-glycerol, or tryptophan, has been detected in these reaction mixtures. Reaction mixtures, prepared by mixing indole, DL-glyceraldehyde-3-phosphate (prepared from the diethylacetal), and highly purified *Neurospora* tryptophan synthetase were incubated at 37°C (*3*). The components and products of the reaction mixture were separated by ascending paper chromatography for an overnight period with a mixture of isopropanol, ammonium hydroxide, and water (100:10:25) as solvent. For two-dimensional chromatograms, a mixture of butanol, acetic acid, and water (60:15:25) was the additional solvent system. Portions of reaction mixtures were compared chromatographically to known standards of indole, indole glycerol phosphate, indole glycerol, tryptophan, serine, and pyridoxal phosphate by scanning with a Mineralight ultraviolet lamp, model SL-2537, and spray-